TRIUMF Experiment E614
Technical Note

An Analysis of Energy Loss in the Proportional Chambers near the Target

M. Grinder and D. H. Wright

31 August 1998

Abstract

Monte Carlo simulations of muon energy loss recorded by the proportional chambers near the target are presented and analyzed. These chambers were found to be very useful in rejecting muon stops just upstream of the target and as a monitor of the muon stopping distribution in the target. It was determined that both ADC's and TDC's are required for the proportional chambers near the target.

Introduction

Two issues vital to the success of E614 may be adressed by the use of four proportional chambers adjacent to the stopping target. The first issue, which affects the muon depolarization, is the removal of events in which muons stop near, but not in, the target. Nominally the trigger condition $\mathrm{PC}(-2) \cdot \mathrm{PC}(-1) \cdot \overline{\mathrm{PC}(+1) \cdot \mathrm{PC}(+2)}$ removes such events. The notation adopted here is that PC(-2), PC(-1) refer to the upstream proportional chambers while PC(+1), PC(+2) refer to the downstream chambers.

However, this simple scheme does not account for those muons that could lose all their energy and stop in PC(-1), nor does it account for those muons that nearly stop in the target and lose a small amount of energy (too little to be detected) in PC(+1). The addition of ADC's to the PC's may solve this first problem, allowing for a measurement of the energy loss. With this information, one can impose cuts that eliminate those muons stopping in PC(-1).

The second issue is the shape of the muon stopping distribution in the target; a symmetric distribution is desired in order to remove the fore-aft asymmetries in the decay positron spectrum. When the upstream mass of the detector is optimized so that the peak of the muon Bragg curve is centered on the target, the stopping distribution is symmetric about $z = 0$. In this case the hit ratios $N_{PC(-1)}/N_{PC(+1)}$, $N_{PC(-2)}/N_{PC(+2)}$ have unique values. If the stopping distribution becomes skewed upstream or downstream, these ratios change significantly, providing a monitor of the shape of the stopping distribution.

Monte Carlo Simulations

Monte Carlo simulations were performed using version 1.0 of the E614 GEANT simulation code. The detector geometry was that adopted at the April 1998 collaboration meeting and consists of, from the stopping target outward: 2 proportional chambers, 22 drift chambers, one plane of plastic scintillator of thickness 340μm, 4 more proportional chambers, and 10 drift chambers for muon tracking.

In the simulation a beam of 29.7 MeV/c μ^+, with a beam divergence of 15 mrad (σ) in x and y and a beamspot of 0.5 cm (σ) in x and y, was started 120 cm upstream of the target. Muons were allowed to decay, but the resulting positrons were not tracked. Finally, a uniform solenoidal field of 2.2 T was oriented along the z-axis.

As muons entered and exited the PC's, their kinetic energy was recorded and their energy loss in each chamber was histogrammed.

The thickness of the plastic scintillator which produced a symmetric stopping distribution in the target was 340 μm. Varying this by $\pm 20\mu$m caused the stopping distribution to be skewed upstream or downstream.

Results

1. Triggers from the Proportional Chambers

The mean energy loss per muon in the chambers was $\sim$0.1 MeV. The distributions of energy loss in PC(-2), PC(-1) ,PC(+1), and PC(+2) are shown in Fig.1.

A scatterplot of energy losses in PC(-2) and PC(-1) is shown in Fig. 2 and exhibits three main features: a dense locus of points with a positive slope, a less dense locus with a negative slope, and two sparse loci of points in which a large energy loss in one chamber is paired with a small energy loss in the other. The dense locus with positive slope is due to muons stopping in the target (Fig. 3, bottom left), and the low energy end of this locus is due to those that pass through the target(Fig. 3, bottom right). The less dense locus of negative slope is due to muons stopping in PC(-1). The points which lie along either axis (those which have large energy loss in one chamber, but small in the other) are due to muons scattering from the PC wires.

As seen in Fig. 3, nearly all stops in PC(-1) have an energy loss in PC(-2) greater than $\sim$0.1 MeV, so a cut at that value would remove most events with stops in PC(-1). A two dimensional cut along the lower edge of the locus of PC(-1) stops would be more efficient, however. The equation of the cut line is approximately $\Delta E(-2) = -1.74 \times \Delta E(-1) + 0.144$ MeV. A cut near this edge will eliminate all the muons stopping in PC(-1), but still leave most of those stopping in the target.

Table I shows the result of various cuts that attempt to minimize stops in PC(-1), but maximize those that stop in the target. The cuts differ only by their x-intercepts. The cut

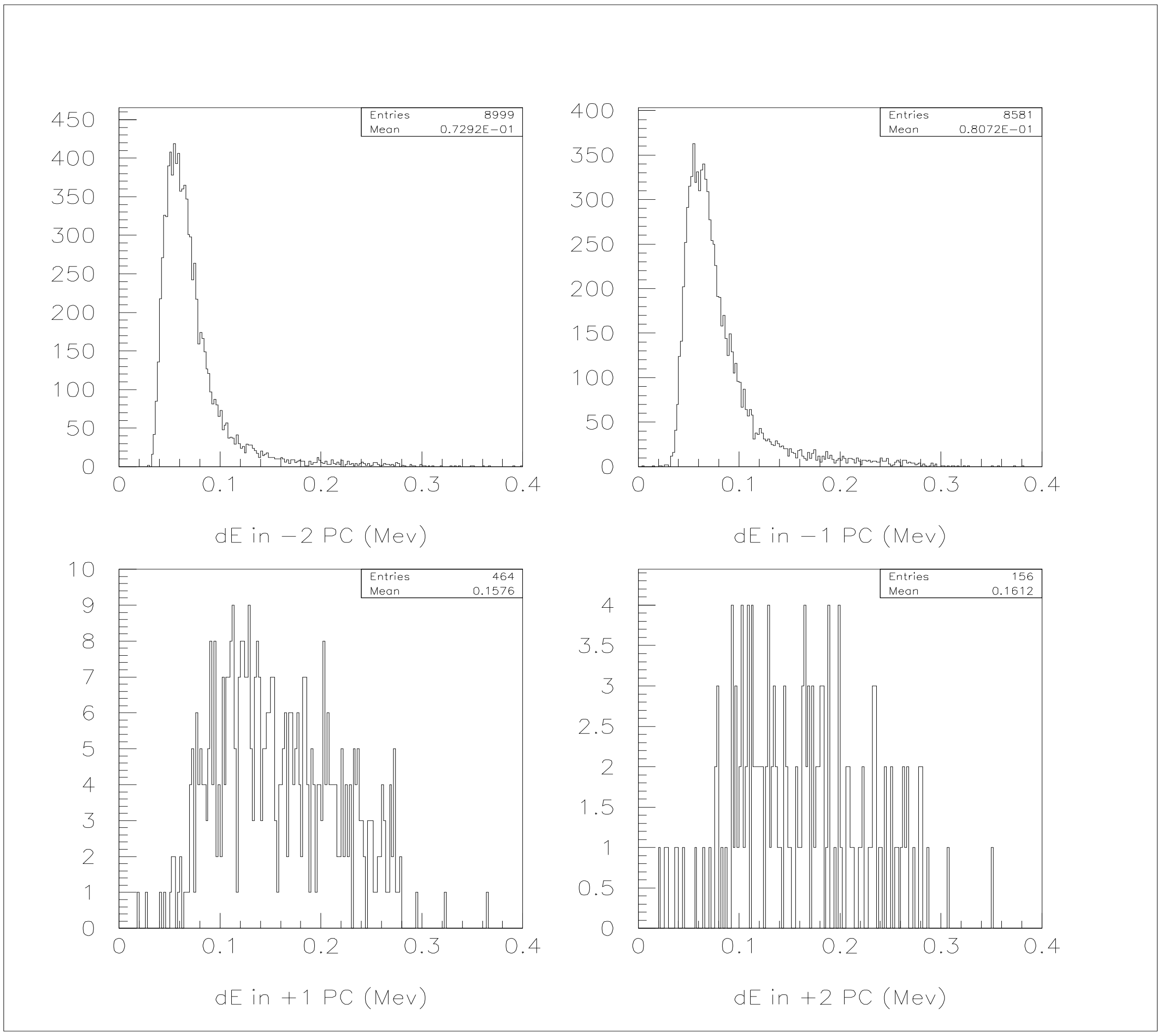

Figure 1: Muon kinetic energy loss in PC(-2),PC(-1),PC(+1), and PC(+2) chambers for an initial 10,000 events.

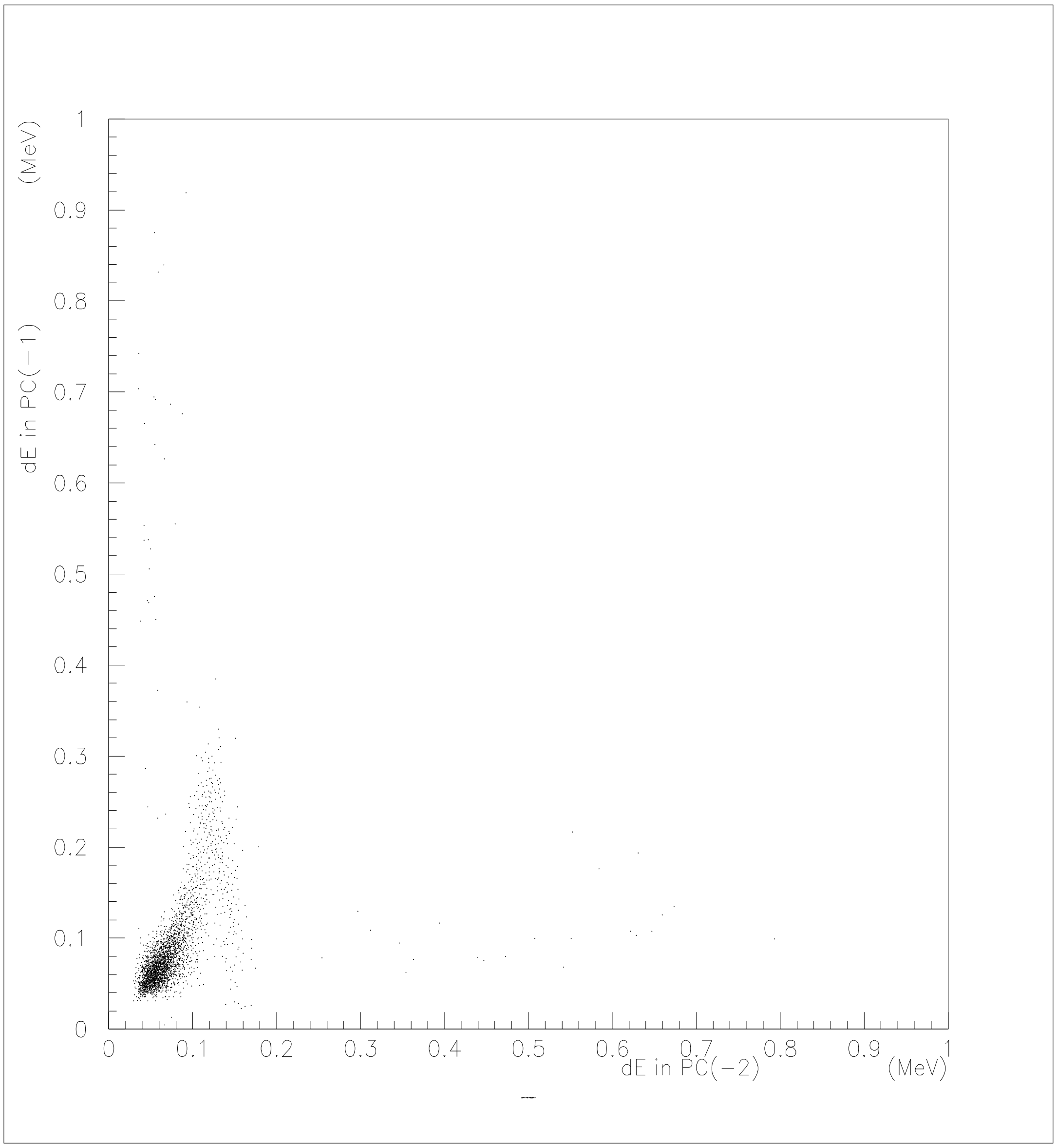

Figure 2: Scatterplot of the kinetic energy loss in PC(-2) and PC(-1) for a symmetric target stopping distribution.

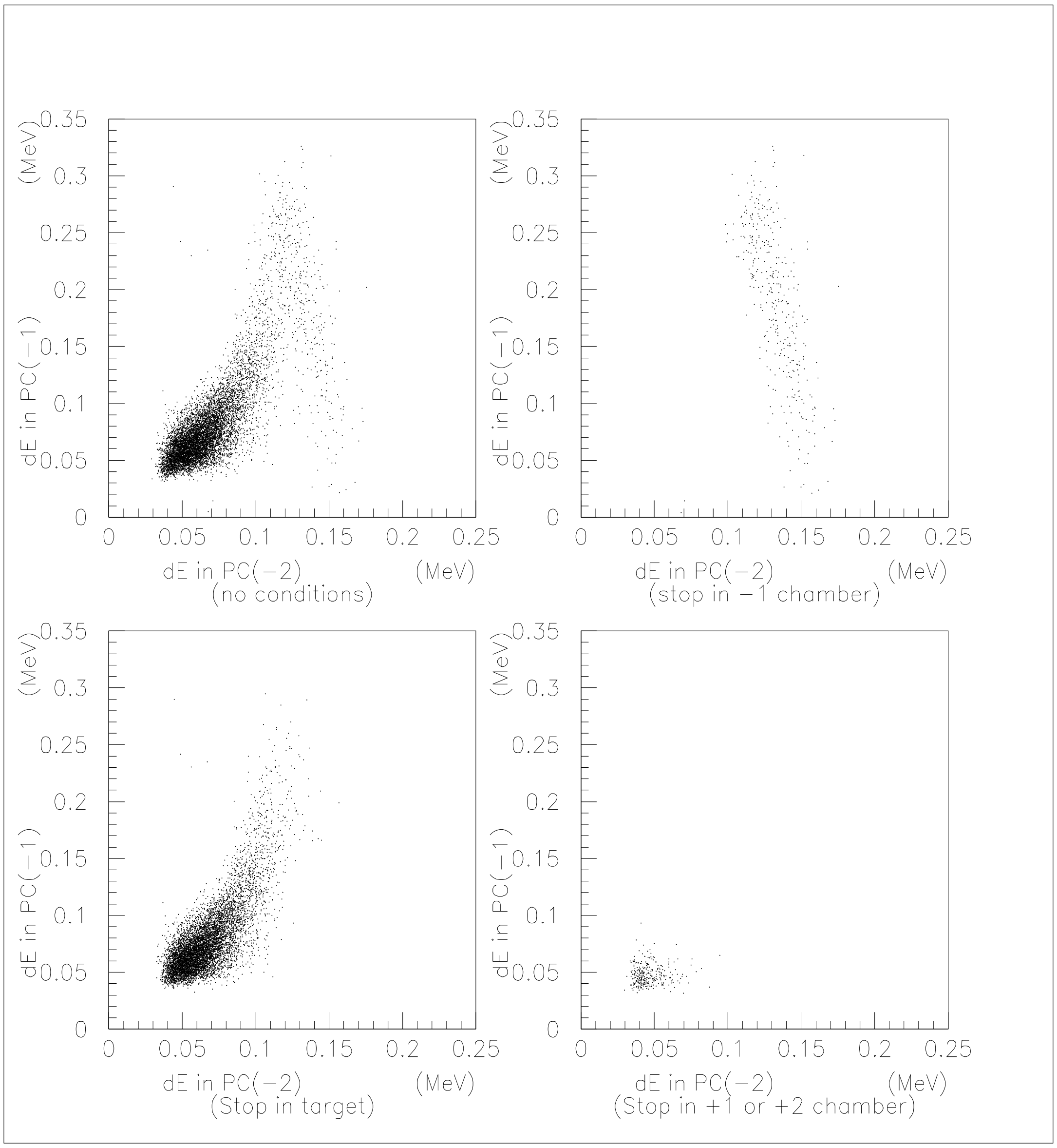

Figure 3: Energy loss in PC(-2) and PC(-1) chambers for various muon stopping conditions. Top left: no conditions; top right: stop in PC(-1); bottom left: stop in target; bottom right: stop in PC(+1) or PC(+2).

at x-intercept = 0.137 MeV eliminates nearly all muons stopping in PC(-1), while leaving more than 97% of the muons stopping in the target. It also removes all events which have large energy loss in PC(-2) and small energy loss in PC(-1). It is also desirable to cut out those muons losing a large amount of energy in PC(-1) due to hits on the sense wires. These were removed by rejecting all events with energy losses in PC(-1) greater than 0.3 MeV and less than 0.03 MeV.

x-intercept of the cut line (MeV)	% stopping in PC(-1)	% stopping in target
0.151	7.3	98.7
0.144	2.3	98.2
0.137	0.6	97.3

Table I. μ^+ stopping percentage in the target and PC(-1) as a function of x-intercept of 2-D cut.

The performance of the proportional chambers, however, has not been simulated here, so it is unclear if the scattering off the wires will appear as shown. The muon may appear to deposit more energy if it scatters off the wire at a large angle and creates more electron showers as it crosses the path of more wires. Otherwise, in a low angle scatter, the energy it loses in the wire will not cause a shower, thus a lower energy signal will be recorded. Therefore, the same sparse loci should be seen, not precisely as shown here, but requiring similar cut values on the energy loss in PC(-1).

It is noted here that the energy threshold of the PC's is at most $\sim$1 keV[1]. From Figs. 1 and 3 (bottom right) it is seen that the smallest energy loss recorded by PC(+1) is $\sim$20 keV. In 10,000 entries, there were no muons that lost less than 1 keV of kinetic energy. Pessimistically assuming that the PC energy threshold is 25 keV, at least 2 in 10^4 events will be lost. Providing the chamber thresholds can be kept low ($\leq$ 5 keV), it is therefore unlikely that muons will pass through the target but not be recorded by PC(+1).

2. Monitoring Stopping Distributions in the Target

A scatterplot of the muon energy losses in PC(-1) and PC(-2) was considered as a monitor of the stopping distribution in the target. In Fig.4 three stopping distributions along with their corresponding energy loss scatterplots are displayed. A symmetric stopping distribution (Fig.4, middle) is produced by placing a 340 μm thick scintillator in the muon path. By decreasing the thickness to 320 μm a stopping distribution skewed toward positive z is produced (Fig.4, top). A skew to negative z is achieved by increasing the thickness to 360 μm (Fig.4, bottom). These scatterplots are very similar and, except for a slight energy displacement, do not show any qualitative difference. The energy displacements suggest mean energy loss as a monitor of stopping distribution. However, this would require precise calibration of the detectors, since differing thresholds, gains, and efficiencies could cause artificial shifts in the mean energy loss.

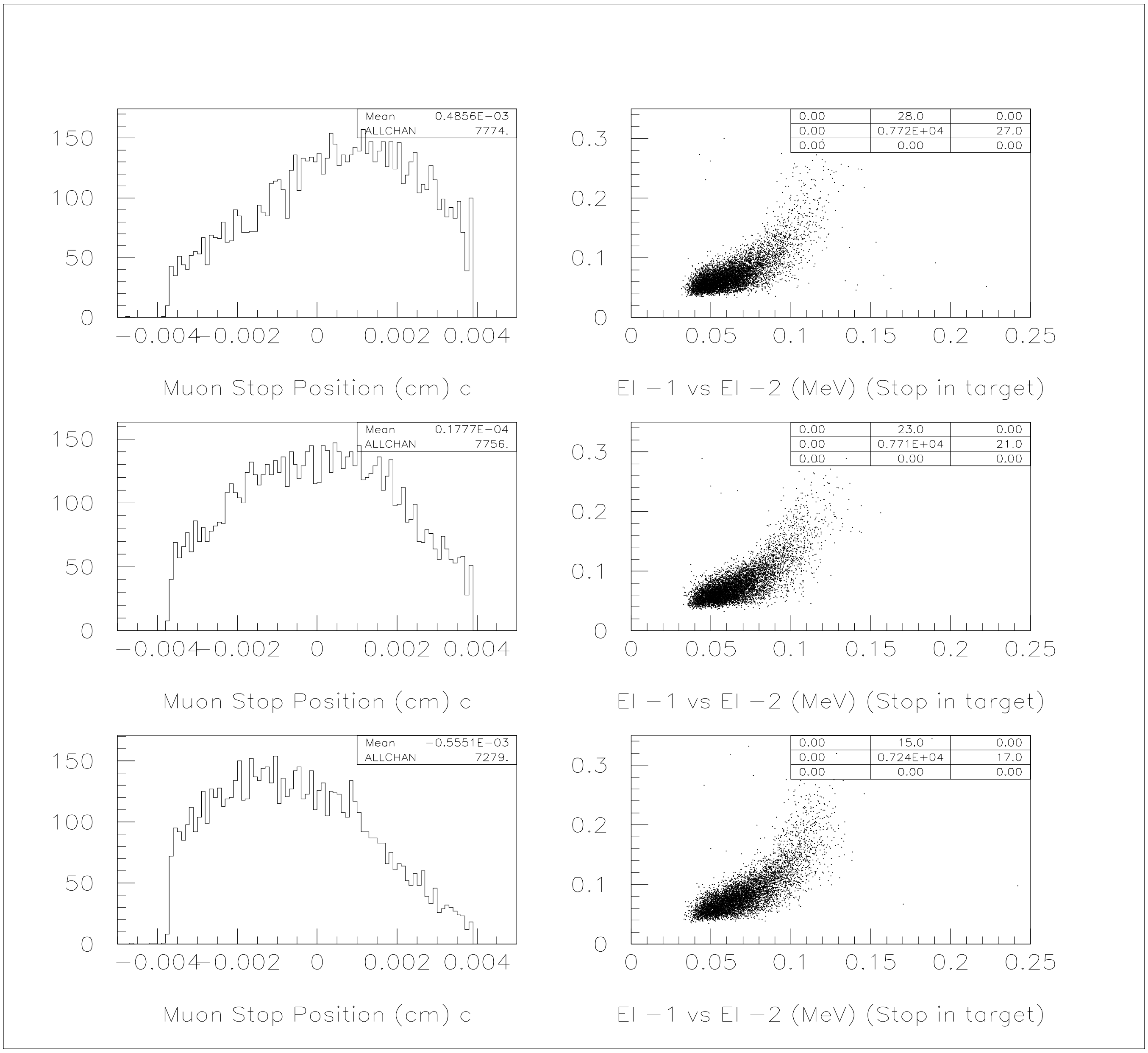

Figure 4: Stopping distribution in the target for a scintillator of thickness 320 μm (top graphs), 340 μm (middle), and 360 μm (bottom). Corresponding scatterplots show energy loss in PC(-1) and PC(-2).

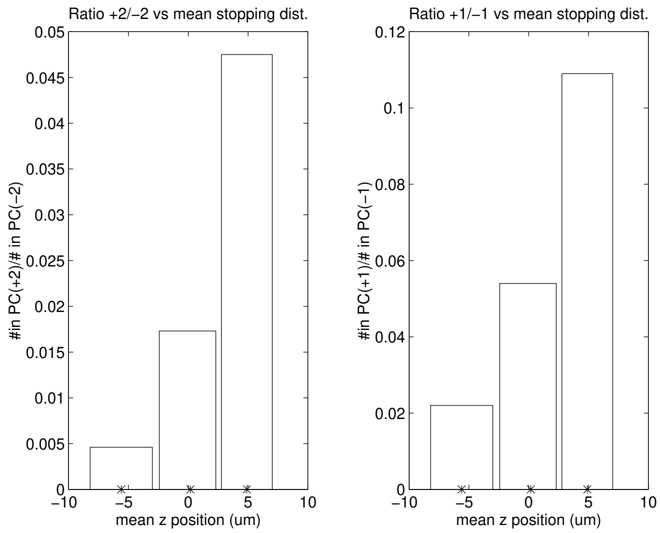

Figure 5: Graphical representation of PC ratios as a function of stopping distribution mean.

A simpler method is merely to count the number of muons passing through the proportional chambers. The ratio of the number of muons recorded by PC(+2) to those recorded by PC(-2), and the ratio of PC(+1) to PC(-1) should change with deviations from a symmetric stopping distribution. These ratios should not be affected by factors such as PC efficiency (unless each chamber has different efficiency) or muons stopping in PC(-1). Other ratios change as well, but $N_{PC(+1)}/N_{PC(-1)}$, and $N_{PC(+2)}/N_{PC(-2)}$ were found to be the most sensitive to changes in the stopping distribution.

stopping distribution	mean in z (μm)	number in PC chamber				Ratios	
		-2	-1	+1	+2	+2/-2	+1/-1
symmetric	0.18	8999	8581	464	156	0.0173 ±0.001	0.054±0.003
right skew	4.9	9327	9021	986	443	0.0475 ±0.002	0.109±0.004
left skew	-5.6	8533	7910	176	39	0.0046 ±0.001	0.022±0.002

Table II. Ratios of number of muons recorded by the proportional chambers as a function of stopping distribution mean.

For a symmetric stopping distribution, table II shows that the ratios, $N_{PC(+1)}/N_{PC(-1)}$, and $N_{PC(+2)}/N_{PC(-2)}$ were 0.054 and 0.0173, respectively. Deviations of $\pm 20\mu$m in scintillator thickness produced a significant change in ratios. These ratios are statistically robust. For example, the ratio $N_{PC(+2)}/N_{PC(-2)}$ for the right-skewed distribution is 16σ different from the same ratio in the symmetric case. These ratios are therefore very sensitive to differences in the stopping distribution, and are shown graphically in Fig.5.

Conclusion

Using ADC's to read out the wires in PC(-2), PC(-1), PC(+1) and PC(+2) provides a means of rejecting events in which muons stop in PC(-1) instead of the target. Making a two dimensional cut on the energy losses in PC(-1) and PC(-2) removes all but 0.6% of such events. The remaining 0.6%, which are due to scattering in the chamber wires, can be reduced by additional cuts. It seems unlikely that muons passing through the target with too little energy to be recorded by PC(+1) will cause a significant error.

The central PC's provide a reliable monitor of stopping distribution when the ratios of the number of muons recorded by PC(+2) and PC(-2) and PC(+1) and PC(-1) are examined.

The above results are largely independent of detector configuration, as long as mass can be added or removed to center the peak of the Bragg curve around $z = 0$.

In sum, the addition of ADC's to the PC chambers, though not required to monitor the stopping distribution in the target, will be a useful means of rejecting false stops near the target.

References

[1] V.I.Selivanov, private communication, 1998.